JOURNAL OF GUIDANCE, CONTROL, AND DYNAMICS
Vol. 24, No. 4, July–August 2001

Stability Analysis of Planetary Satellite Orbiters: Application to the Europa Orbiter

D. J. Scheeres*
University of Michigan, Ann Arbor, Michigan 48109-2140
M. D. Guman†
Jet Propulsion Laboratory, California Institute of Technology, Pasadena, California 91109-8099
and
B. F. Villac‡
University of Michigan, Ann Arbor, Michigan 48109-2140

The stability of orbit dynamics around a planetary satellite is studied using analytical and numerical techniques. The Europa orbiter mission is used to motivate our analysis and to provide specific numerical data for verification of our analytical results. After verification, the results are applied to a large number of planetary satellites in the solar system. The motivation is that numerically integrated, low-altitude spacecraft orbits about Europa often impact on that moon's surface after a short period of a few days to weeks. Numerical integrations indicate that these impact orbits only occur for inclinations within ~45 deg of a polar orbit. An analytical study of this problem using averaging theory, which results in an approximate, closed-form solution for the orbiter dynamics, is described. The solution includes the effect of the planet gravity and the planetary satellite oblateness, with the assumption that the eccentricity of the nominal orbit is small. This solution is used to compute limits for impacting and nonimpacting orbits at Europa and provides good agreement with numerical computations of these limits performed with high-precision numerical integrations of the motion. The analytical result predicts a set of initial conditions that can postpone impact with the planetary surface for considerable lengths of time.

Introduction

THE orbit dynamics of low-altitude, near-circular orbits above a planetary satellite are studied. The mathematical model used in the analysis includes the tidal force from the planet and the effect of the planetary satellite's oblateness. As such, our model problem corresponds to the investigation of a particular region of initial condition space of the classical Hill problem (see Ref. 1), with the modification of an oblate central body. Hill's approximation was initially introduced to solve the problem of the motion of the moon (see Ref. 2), but in actuality has a much more general realm of application (see Ref. 3). An extensive numerical investigation of the Hill problem was given by Hénon,[4] and previous applications of the Hill approximation have included the study of orbit dynamics in the vicinity of asteroids (see Refs. 5 and 6). However, these previous investigations have not considered motion in the realm in which low-altitude, planetary satellite orbiters fall.

The motivation for the study reported here is the observation that numerically integrated low-altitude spacecraft orbits about Europa with inclinations within ~45 deg of polar suffer impacts with that planetary satellite's surface in time spans of days to weeks. To explain this dynamic instability, we have formulated an approximate, averaged model for the motion of a satellite about Europa.[7] The theory is general enough, however, to apply to a wide range of low-altitude orbits about planetary satellites and, thus, is formulated in a general fashion that allows extension of the results to these other cases.

In our analysis we show that the secular motion for low-altitude, planetary satellite orbiters can be solved in closed form and provides an accurate characterization of orbit stability. The theory predicts regions of unstable circular orbits for a range of near-polar inclinations. Inclusion of satellite oblateness effects on the dynamics modifies these intervals of instability, and in the limit when the secular effect of the oblateness is much larger than the secular effect of the tide, the intervals of unstable circular orbits are restricted to the vicinity of the critical inclinations in the main problem of satellite orbiters. Our approximate theory is validated by a comparison of results with precision numerical integrations performed for the Europa orbiter mission. From the analytical theory, we find a special set of initial conditions that can extend the life of an unstable orbiter, and we validate these solutions numerically. Finally, we consider the application of the current result to all known planetary satellites of possible interest in the solar system, along with indications of the applicability of the model assumptions. This final series of computations highlights the value of an analytical understanding of the instability because it allows our result to be immediately applied to a range of problems.

Received 27 March 2000; revision received 8 January 2001; accepted for publication 10 January 2001.

*Assistant Professor of Aerospace Engineering; scheeres@umich.edu. Senior Member AIAA.
†Engineering Staff, Navigation and Mission Design Section; mark.guman@jpl.nasa.gov. Senior Member AIAA.
‡Graduate Student, Department of Aerospace Engineering; bvillac@engin.umich.edu.

Dynamics of Planetary Satellite Orbiters

Perturbation Models

The physical situation modeled consists of a spacecraft in a low-altitude, near-circular orbit around a planetary satellite that is in orbit about a larger planet (Fig. 1). Formally, this can be written as a restricted three-body problem (assuming the planetary satellite is in a circular orbit). However, this physical situation also has all of the elements necessary to apply the Hill approximation (see Ref. 3). Specifically, we may assume that the planetary satellite is in a near-circular orbit about the primary, that the orbiter is in a tightly bound, that is, low-altitude, orbit about the planetary satellite, and that the mass of the planetary satellite is sufficiently small compared to the planet's mass. The last condition is stated specifically as $(M_S/M_P)^{1/3} \ll 1$ and allows us to expand the effect of the planet's gravitational attraction up to second order in this small parameter. For the Europa–Jupiter system, this parameter equals ~0.03, indicating the validity of the smallness assumption.

Then, the perturbing effect of the planet's gravity can be stated in potential form as[8]

$$\mathcal{R} = \tfrac{3}{2}N_S^2x^2 - \tfrac{1}{2}N_S^2r^2 \tag{1}$$

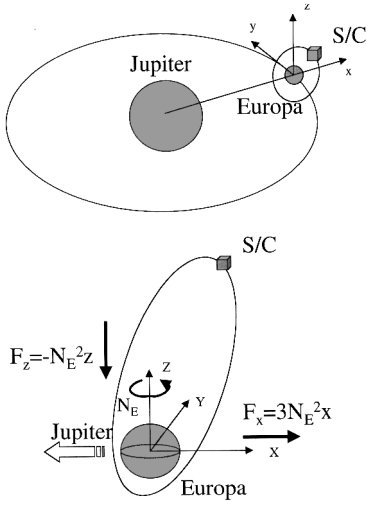

Fig. 1 Geometry of the Europa orbiter model.

where x is measured along the line from the planet to its satellite, r is the orbital radius from the satellite center, and N_S is the orbit angular rate of the planetary satellite about the planet (see Fig. 1 for the coordinate geometry). The equations of motion of the orbiter can then be specified in the Cartesian frame rotating with the planetary satellite about the planet:

$$\ddot{x} - 2N_S\dot{y} = -\frac{\mu_S}{r^3}x + N_S^2 x + \frac{\partial \mathcal{R}}{\partial x} = -\frac{\mu_S}{r^3}x + 3N_S^2 x$$

$$\ddot{y} + 2N_S\dot{x} = -\frac{\mu_S}{r^3}y + N_S^2 y + \frac{\partial \mathcal{R}}{\partial y} = -\frac{\mu_S}{r^3}y$$

$$\ddot{z} = -\frac{\mu_S}{r^3}z + \frac{\partial \mathcal{R}}{\partial z} = -\frac{\mu_S}{r^3}z - N_S^2 z \tag{2}$$

where μ_S is the gravitational parameter of the attracting satellite, x is measured from the planetary satellite center away from the planet, z is measured from the planetary satellite center out of its orbital plane, y completes the triad and points in the direction of the planetary satellite's motion, and $r = \sqrt{(x^2 + y^2 + z^2)}$. For theoretical discussions involving the Hill equations, all of the parameters in the equations are usually removed by scaling the time by $1/N_S$ and the position by $(\mu_S/N_S^2)^{1/3}$. We do not perform such a rescaling, however, because this would obscure the specific application being made here.

In terms of inertially referenced orbital elements, the coordinate x is

$$x = r[\cos(\omega + \nu)\cos(\tilde{\Omega}) - \sin(\omega + \nu)\sin(\tilde{\Omega})\cos i] \tag{3}$$

$$\tilde{\Omega} = \Omega - N_S(t - t_0) \tag{4}$$

where ω is the argument of periapsis, ν is the true anomaly, i is the inclination, Ω is the longitude of the ascending node relative to an inertial frame, t is the time, t_0 is an initial epoch, and $\tilde{\Omega}$ is the longitude of the ascending node relative to the rotating coordinate frame. Using these definitions, we can express the perturbing potential in terms of osculating orbital elements alone:

$$\mathcal{R} = \left(N_S^2 r^2/2\right)\{3[\cos(\omega+\nu)\cos(\tilde{\Omega}) - \sin(\omega + \nu)\sin(\tilde{\Omega})\cos i]^2 - 1\} \tag{5}$$

It then becomes possible to use this potential in the Lagrange planetary equations[8] to compute the effect of the tidal force on the osculating orbital elements.

Averaging Assumptions

To simplify the analysis of this problem, we concentrate only on secular changes in the orbital elements. The secular effect of the tidal perturbation can be found by averaging the perturbing potential over the orbit mean anomaly and then substituting this averaged potential into the Lagrange equations.[8] We note that the perturbing potential, as expressed in inertial orbital elements, has a time variation in the longitude of the ascending node corresponding to the motion of the planetary satellite about the planet. Thus, in addition to the smallness assumption of the perturbing force (which is valid here, in general), we also assume that the orbiter's mean motion about the planetary satellite, $n = \sqrt{(\mu_S/a^3)}$, where a is the semimajor axis of the spacecraft, is much greater than the planetary satellite's mean motion N_S. This then implies that in the time it takes the orbiter to make one revolution about the satellite, the satellite will only have moved a relatively small angle about the planet. The ratio of Europa's mean motion over a low-altitude Europa orbiter's mean motion is $\sim$0.02, implying that Europa will move an angle of only 7 deg over one period of the orbiter.

Thus, we first average the potential over one spacecraft orbit, assuming that $\tilde{\Omega}$ (or the term $N_S t$) is constant:

$$\bar{\mathcal{R}} = \frac{1}{2\pi}\int_0^{2\pi} \mathcal{R}\, \mathrm{d}M \tag{6}$$

where the averaging is performed with respect to the mean anomaly of the orbiter ($M = nt$). To apply the averaging, we transform from mean anomaly to true anomaly and write the averaged potential as

$$\bar{\mathcal{R}} = \frac{1}{2\pi}\frac{a^2(1-e^2)^4 N_S^2}{4\sqrt{1-e^2}}\int_0^{2\pi}\frac{1}{(1+e\cos f)^4}[(1 - 3\sin^2\tilde{\Omega}\sin^2 i)$$

$$+ 3(\cos 2\tilde{\Omega} + \sin^2\tilde{\Omega}\sin^2 i)\cos 2(f+\omega)$$

$$- 3\sin 2\tilde{\Omega}\cos i\sin 2(f+\omega)]\,\mathrm{d}f \tag{7}$$

The expression $1/(1+e\cos f)^4$ can be expanded as a cosine series:

$$\frac{1}{(1+e\cos f)^4} = \sum_{m=0}^{\infty} b_m \cos(mf) \tag{8}$$

where closed-form expressions of its coefficients are given in Ref. 9. Of specific interest are the coefficients

$$b_0 = \frac{\sqrt{1-e^2}}{(1-e^2)^4}\left(1 + \frac{3}{2}e^2\right) \tag{9}$$

$$b_2 = 5\frac{\sqrt{1-e^2}}{(1-e^2)^4}e^2 \tag{10}$$

With these results, the quadrature can be completed to find

$$\bar{\mathcal{R}} = \left(N_S^2 a^2/4\right)\left\{\left(1 - \tfrac{3}{2}\sin^2 i + \tfrac{3}{2}\cos 2\tilde{\Omega}\sin^2 i\right)\left(1 + \tfrac{3}{2}e^2\right)\right.$$

$$+ \tfrac{15}{4}e^2\cos 2\omega[\sin^2 i + \cos 2\tilde{\Omega}(1 + \cos^2 i)]$$

$$\left. - 5e^2\sin 2\omega\sin 2\tilde{\Omega}\cos i\right\} \tag{11}$$

Although the averaged potential is now simplified, it still has a time-varying term $\tilde{\Omega}$ due to the motion of the planetary satellite. A further simplification can be made by averaging the potential over one orbit about the planet. For the Europa orbiter problem, this second averaging is justified because there are order of magnitude differences between the period of the Europa orbiter and the period of Europa about Jupiter, and between the period of the Europa orbit about Jupiter (3.5 days) and the timescale of the instability of the Europa orbiters ($\sim$1 + month). This second averaging is motivated more by intuitive reasoning than by mathematical argument. It is similar in spirit to the method used by Gauss in computing secular variations due to a perturbing planet, by replacing the planet with an elliptical ring.[10] Later we will justify this approach by comparing the results of our analysis with precision numerical integrations and by relating the timescale assumption to the earlier averaging

assumption of $N_S/n \ll 1$. Performing this second averaging yields a time-invariant potential:

$$\tilde{\mathcal{R}} = \frac{1}{2\pi}\int_0^{2\pi} \bar{\mathcal{R}}\, \mathrm{d}(N_S t) \tag{12}$$

$$\tilde{\mathcal{R}} = \frac{N_S^2 a^2}{4}\left[\left(1-\frac{3}{2}\sin^2 i\right)\left(1+\frac{3}{2}e^2\right)+\frac{15}{4}e^2\cos 2\omega \sin^2 i\right] \tag{13}$$

Because we are considering the dynamics of a low-altitude orbiter, the effect of planetary satellite oblateness may also be an important element. The form of this perturbing potential can be averaged over a single orbit to yield[11]

$$\bar{\mathcal{R}}_{J_2} = \frac{\mu_S J_2}{2a^3(1-e^2)^{\frac{3}{2}}}\left(1-\frac{3}{2}\sin^2 i\right) \tag{14}$$

where J_2 is the Europa oblateness term, given here in length units squared. This perturbing potential can be added to the doubly averaged tidal perturbation potential to yield our final, secular, perturbing potential.

Secular Lagrange Equations

We now use the doubly averaged potential in the Lagrange planetary equations[8] to find the secular equations of these elements. We first state these equations incorporating only the tidal term [Eq. (13)]:

$$\frac{\mathrm{d}a}{\mathrm{d}t} = 0 \tag{15}$$

$$\frac{\mathrm{d}i}{\mathrm{d}t} = -\frac{15}{16}\frac{N_S^2}{n}\frac{e^2}{\sqrt{1-e^2}}\sin 2i \sin 2\omega \tag{16}$$

$$\frac{\mathrm{d}\Omega}{\mathrm{d}t} = -\frac{3}{8}\frac{N_S^2}{n}\frac{\cos i}{\sqrt{1-e^2}}(2+3e^2-5e^2\cos 2\omega) \tag{17}$$

$$\frac{\mathrm{d}e}{\mathrm{d}t} = \frac{15}{8}\frac{N_S^2}{n}e\sqrt{1-e^2}\sin^2 i \sin 2\omega \tag{18}$$

$$\frac{\mathrm{d}\omega}{\mathrm{d}t} = \frac{3}{8}\frac{N_S^2}{n}\frac{1}{\sqrt{1-e^2}}[5\cos^2 i - 1 + 5\sin^2 i\cos 2\omega + e^2(1-5\cos 2\omega)] \tag{19}$$

We note that the semimajor axis is constant, as is the usual case for secular perturbations arising from a force potential. We also note that the longitude of the ascending node, Ω, is ignorable in that its motion does not affect any other secular element. Similarly, the modification of the mean anomaly is ignorable and is not presented here. Thus, the secular effect of the tidal perturbation creates a coupled evolution of the orbit inclination, eccentricity, and argument of periapsis.

Because we will only be considering low-altitude orbiters, we can restrict our analysis to small eccentricities. Specifically, if we assume the semimajor axis of the orbit is expressed as $R_S + h$, where R_S is the satellite radius and h is the altitude, then the eccentricity of the orbit is constrained by

$$e < h/(R_S + h) \tag{20}$$

which is small, given our assumption on h. Neglecting higher orders of eccentricity in the coupled motion of i, e, and ω, we find

$$\frac{\mathrm{d}i}{\mathrm{d}t} \sim \mathcal{O}(e^2) \tag{21}$$

$$\frac{\mathrm{d}e}{\mathrm{d}t} \sim \frac{15}{8}\frac{N_S^2}{n}e\sin^2 i \sin 2\omega + \mathcal{O}(e^2) \tag{22}$$

$$\frac{\mathrm{d}\omega}{\mathrm{d}t} \sim \frac{3}{8}\frac{N_S^2}{n}(4-5\sin^2 i + 5\sin^2 i\cos 2\omega) + \mathcal{O}(e^2) \tag{23}$$

Thus, the inclination should be constant on average [to $\mathcal{O}(e)$], reducing this to a two-dimensional problem.

At this point, we can incorporate the effect of the planetary satellite oblateness into the analysis. From classical analyses of the J_2 effect on low-altitude orbits, we note that, on average, the semimajor axis, inclination, and eccentricity will not be affected and that the longitude of the ascending node and argument of periapsis will have a constant secular change due to this term. As before, the longitude of the ascending node is ignorable because it has no effect on the remaining elements; thus, we do not consider this term. The effect of J_2 on the argument of periapsis is represented as

$$\dot{\omega}_{J_2} = \left[3nJ_2/a^2(1-e^2)^2\right]\left(1-\tfrac{5}{4}\sin^2 i\right) \tag{24}$$

Including the effect of J_2 on the argument of periapsis and ignoring higher orders of eccentricity yields the final form of the secular Lagrange equations:

$$\frac{\mathrm{d}e}{\mathrm{d}t} = \frac{15}{8}\frac{N_S^2}{n}e\sin^2 i \sin 2\omega \tag{25}$$

$$\frac{\mathrm{d}\omega}{\mathrm{d}t} = \frac{3}{8}\frac{N_S^2}{n}(4-5\sin^2 i + 5\sin^2 i\cos 2\omega) + \frac{3nJ_2}{p^2}\left(1-\frac{5}{4}\sin^2 i\right) \tag{26}$$

For notational convenience, we rewrite the equation for the argument of periapsis as

$$\dot{\omega} = \frac{15}{8}\frac{N_S^2}{n}\sin^2 i(\cos 2\omega + \alpha) \tag{27}$$

$$\alpha = (1+2\epsilon)\frac{4-5\sin^2 i}{5\sin^2 i} \tag{28}$$

$$\epsilon = \left(\frac{n}{N_S}\right)^2\left(\frac{J_2}{a^2}\right) \tag{29}$$

This form of the equation is valid only for nonequatorial orbits ($i \neq 0, \pi$), but neither of these inclinations will be considered in our analysis. For the Europa orbiter, the parameter $\epsilon \sim 0.47$ for an altitude of 200 km. We note that the parameter ϵ is not necessarily small. For example, the same quantity evaluated for a low-Earth orbiter considering the tidal perturbation of the sun yields a value of $\epsilon \sim 1.9 \times 10^4$; for a geosynchronous orbit it yields a value of $\epsilon \sim 3$.

Analytical Integration of the Equations

Equation (27) for the argument of periapsis can be reduced to quadratures because it contains only terms that are functions of itself. Carrying out this integration yields the explicit solution

$$\tan\omega = \begin{cases} \left[\sqrt{(1+\alpha)/(1-\alpha)}\right]\tanh(\lambda t+\phi) & \alpha^2<1 \\ \lambda t + \tan(\omega_0) & \alpha = 1 \\ \left[\sqrt{(\alpha+1)/(\alpha-1)}\right]\tan(\lambda t+\phi) & \alpha^2>1 \end{cases} \tag{30}$$

$$\lambda = \begin{cases} \frac{15}{8}\left(N_S^2/n\right)\sin^2 i\sqrt{1-\alpha^2} & \alpha^2<1 \\ \frac{15}{4}\left(N_S^2/n\right)\sin^2 i & \alpha = \pm 1 \\ \frac{15}{8}\left(N_S^2/n\right)\sin^2 i\sqrt{\alpha^2-1} & \alpha^2>1 \end{cases} \tag{31}$$

$$\phi = \begin{cases} \tanh^{-1}\left\{\left[\sqrt{(1-\alpha)/(1+\alpha)}\right]\tan(\omega_0)\right\} & \alpha^2<1 \\ \tan^{-1}\left\{\left[\sqrt{(\alpha-1)/(\alpha+1)}\right]\tan(\omega_0)\right\} & \alpha^2>1 \end{cases} \tag{32}$$

Note that the solution for the case $\alpha < 1$ can also be described by replacing all instances of tanh with coth, either one yielding an appropriate solution. This duality exists to allow all possible values of ω to occur. Similarly, for the case when $\alpha = -1$, the functions $\tan(\omega)$ can be replaced with $\cot(\omega)$.

This result clearly shows different behavior as a function of the parameter α. Specifically, for $\alpha^2 < 1$, the argument of periapsis approaches the limiting value

$$\omega = \tan^{-1}\sqrt{(1+\alpha)/(1-\alpha)} \tag{33}$$

whereas for $\alpha^2 > 1$, the argument of periapsis circulates.

Given this solution for ω, it is possible to reduce the differential equation for e to quadratures as well. This separated equation can also be integrated in closed form:

$$e = \begin{cases} e_0\sqrt{\dfrac{\cosh 2(\lambda t+\phi)-\alpha}{\cosh 2\phi-\alpha}} & \alpha^2 < 1 \\ e_0\sqrt{\dfrac{1+(\tan\omega_0+\lambda t)^2}{1+\tan\omega_0^2}} & \alpha = 1 \\ e_0\sqrt{\dfrac{\alpha-\cos 2(\lambda t+\phi)}{\alpha-\cos 2\phi}} & \alpha^2 > 1 \end{cases} \tag{34}$$

Again, we note a change in solution properties as a function of the parameter α. When $\alpha^2 > 1$, the eccentricity will oscillate, whereas when $\alpha^2 < 1$, the eccentricity will grow exponentially. Thus, we see explicitly that it is possible for eccentricity to evolve in an unstable fashion, which could lead to impact of a low-altitude orbit with the planetary satellite surface. For our case, impact with the surface will usually preceed eccentricity becoming so large as to violate the smallness assumptions made earlier.

Solution in Terms of h and k

Although the derivation of the solution is simpler in terms of orbital elements ω and e, the form and interpretation of the solution is eased in terms of the orbit elements:

$$h = e\sin\omega \tag{35}$$

$$k = e\cos\omega \tag{36}$$

For $\alpha^2 < 1$ we find

$$h = \left(e_0/\sqrt{1-\alpha}\right)\left[\sqrt{1+\alpha}\cos\omega_0\sinh(\lambda t) + \sqrt{1-\alpha}\sin\omega_0\cosh(\lambda t)\right] \tag{37}$$

$$k = \left(e_0/\sqrt{1+\alpha}\right)\left[\sqrt{1+\alpha}\cos\omega_0\cosh(\lambda t) + \sqrt{1-\alpha}\sin\omega_0\sinh(\lambda t)\right] \tag{38}$$

whereas for $\alpha^2 > 1$ we find

$$h = \left(e_0/\sqrt{\alpha-1}\right)\left[\sqrt{\alpha+1}\cos\omega_0\sin(\lambda t) + \sqrt{\alpha-1}\sin\omega_0\cos(\lambda t)\right] \tag{39}$$

$$k = \left(e_0/\sqrt{\alpha+1}\right)\left[\sqrt{\alpha+1}\cos\omega_0\cos(\lambda t) + \sqrt{\alpha-1}\sin\omega_0\sin(\lambda t)\right] \tag{40}$$

and, for $\alpha = 1$, the system degenerates to

$$h = e_0(\sin\omega_0 + \lambda t\cos\omega_0) \tag{41}$$

$$k = e_0\cos\omega_0 \tag{42}$$

Figure 2 shows the evolution of eccentricity and argument of periapsis for the main cases. For $\alpha^2 > 1$, circular orbits correspond to stable, fixed points of the secular equations. Conversely, for $\alpha^2 < 1$, circular orbits correspond to unstable, fixed points of the secular equations. Thus, the system and solutions can also be viewed in context of the stability of circular orbits at low altitudes.

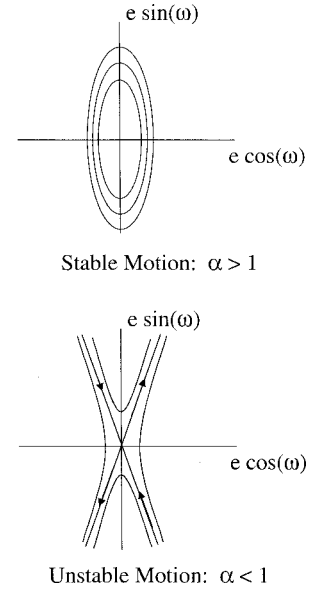

Fig. 2 Stable and unstable orbit solutions.

Stability and Time to Impact

From our solution, we can explicitly determine the stability conditions for an orbiter, and for the unstable case, we can determine the time to impact. The stability condition is obviously $\alpha^2 > 1$, which can be reduced to a set of limits on the inclination of the orbiter:

$$\sin^2 i < \tfrac{2}{5}[(1+2\epsilon)/(1+\epsilon)] \tag{43}$$

or

$$\sin^2 i > \tfrac{2}{5}[(1+2\epsilon)/\epsilon] \tag{44}$$

We note that the ϵ term is due to the oblateness of the planetary satellite and involves the semimajor axis of the orbit and the mean motion of the planetary satellite about the planet. The second condition cannot occur if $\epsilon < 2$, meaning that it does not come into play for the Europa orbiter; however, it does come into play for planetary orbiters where (as noted) the values of ϵ can become large. If the oblateness term is neglected ($\epsilon \sim 0$), the stability condition becomes independent of physical parameter values and reduces to

$$\sin^2 i < \tfrac{2}{5} \tag{45}$$

which corresponds to inclinations in the regions $0 \le i < 39.23$ and $140.77 < i \le 180$. As ϵ increases from zero, the range of these stability intervals will increase.

For $\epsilon > 2$ the second condition [Eq. (44)] becomes active and creates an additional stability region symmetrically placed about a polar orbit ($i = 90$ deg). If $\epsilon \gg 1$, then these stability intervals approach each other and leave the stability condition as $\sin^2 i \neq 4/5$. This situation occurs when N_S is extremely small, such as a planet orbiting about the sun where the period is on the order of years or when the J_2 perturbation dominates over the tidal perturbation. Thus, the analogous eccentricity instability for a low-Earth orbiter would lie in small intervals around the critical inclinations of 63.43 and 116.56 deg. For a geosynchronous orbit where $\epsilon \sim 3$, this interval of unstable inclinations would range from 56.8 to 75 deg and from 105 to 123.2 deg. Note, however, that the time constant of this instability for an orbiter about the Earth will be extremely long, on the order of 39 years for a geosynchronous satellite. In the remainder of the paper we will only consider the case when $\epsilon < 2$, effectively eliminating planetary orbiters from consideration.

The solution for eccentricity can also predict the time to impact for an unstable orbiter. Assume a near-circular orbit above the planetary satellite with semimajor axis $a = h + R_S$, where h is the altitude and R_S is the radius of the planetary satellite (or the top of its atmosphere). Because the semimajor axis is constant on average,

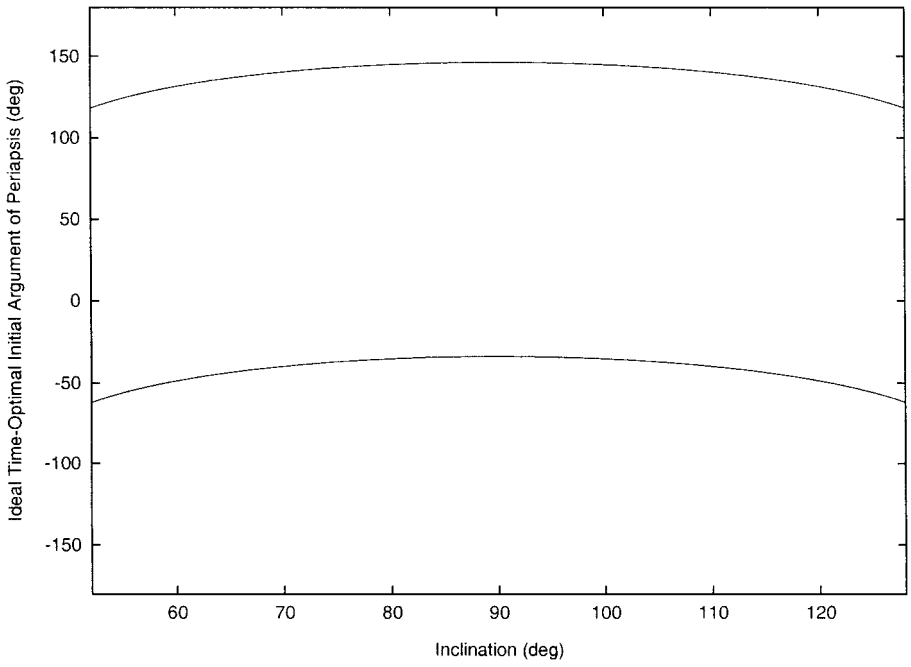

Fig. 3 Time-to-impact optimal initial argument of periapsis plotted as a function of inclination for a 200-km altitude orbiter.

the condition for impact is that the periapsis radius drops below R_S, or $a(1-e) \leq R_S$. Solving for the eccentricity at impact yields

$$e_{\text{imp}} = h/(R_S + h) \tag{46}$$

Then, from Eq. (34), the corresponding time to impact can be explicitly computed as

$$T_{\text{imp}} = (1/2\lambda)\left\{\cosh^{-1}\left[\alpha + (e_{\text{imp}}/e_0)^2(\cosh 2\phi - \alpha)\right] - 2\phi\right\} \tag{47}$$

This gives an explicit prediction of impact time as a function of initial eccentricity, orbit altitude, inclination, and argument of periapsis.

An interesting phenomenon can be noted in Eq. (34) because, by inspection of Eq. (47), we can deduce that the time to impact can be maximized by choosing $\phi \to -\infty$. With this value for an initial condition, we see that it will, ideally, take an infinite length of time for the ratio e/e_0 to increase. The condition for $\phi \to -\infty$ is

$$\tan\omega_0 = -\sqrt{(1+\alpha)/(1-\alpha)} \tag{48}$$

$$\tan\omega_0 = -\tan\omega_{\text{lim}} \tag{49}$$

$$\omega_0 = -\omega_{\text{lim}}, \pi - \omega_{\text{lim}} \tag{50}$$

Thus, choosing the initial argument of periapsis according to this relation can theoretically increase the time to impact of the orbiter. Figure 3 plots these optimal initial arguments of periapsis as a function of inclination for an orbiter about Europa at a 200-km altitude.

In terms of the elements h and k, the solution for this special case reduces to

$$h^* = \mp\left(e_0/\sqrt{2}\right)\sqrt{1+\alpha}\,e^{-\lambda t} \tag{51}$$

$$k^* = \pm\left(e_0/\sqrt{2}\right)\sqrt{1-\alpha}\,e^{-\lambda t} \tag{52}$$

The argument of periapsis is

$$\tan\omega^* = h^*/k^* = -\sqrt{(1+\alpha)/(1-\alpha)}$$

and does not change from its initial value. The eccentricity becomes

$$e^* = \sqrt{h^{*2} + k^{*2}} = e_0 e^{-\lambda t} \tag{53}$$

and asymptotically reduces to zero.

Even though this particular solution is asymptotically stable to a zero eccentricity, the neighborhood of this solution does not have this stability property, and, in fact, small perturbations will excite the unstable manifold and cause the eccentricity to eventually increase exponentially in time. Thus, whereas it is possible to use this result to gain additional time before an impact occurs, an uncontrolled orbit will eventually become unstable and impact. Should active control of the orbit be possible, a reasonable approach (based on this solution) would be to occasionally reset the orbit argument of periapsis to a value close to this asymptotic solution.

Comparison of Analytical and Numerical Solutions for the Europa Orbiter

The basic results from the analytical solution described earlier are verified by making comparisons between the analytical results, the results of numerical integrations of the approximate model, and the results of the precision numerical integration program DPTRAJ. For our test case we use the Europa orbiter mission profile, which nominally puts the spacecraft into a near-polar orbit with an altitude of 200 km. The Appendix contains brief descriptions of the force models used in the approximate model and in the DPTRAJ program. Comparisons between the analytic solution and high-precision numerical integrations incorporating all relevant perturbations acting on the spacecraft are made. Additionally, some comparisions are made between numerical integrations of the simplified model [Eqs. (2)], the analytical solution, and the DPTRAJ solutions.

Stability Limits of the Europa Orbiter

Figure 4 shows the line along which $\alpha = 1$ as a function of inclination and orbiter altitude for the Europa constants. Stability regions were also generated with DPTRAJ for a range of initial orbit elements of the spacecraft relative to Europa, including altitudes ranging from 100 to 400 km and inclinations ranging from 0 to 180 deg. Eccentricity, longitude of ascending node, argument of periapsis, and time past periapsis were all given initial values of zero. Trajectories were integrated for 1 year past the initial epoch, unless the spacecraft impacted the surface of Europa. All of the impact cases in this analysis occurred within 9 months of the initial epoch. These results are also shown in Fig. 4. Additional cases were also run that varied the initial values of the longitude of the ascending node and argument of periapsis over their intervals of definition and the eccentricity over a range of small, near-circular values. Although impact times changed for these cases, the stability regions were consistent with Fig. 4. As is clear from the plot, the regions of stability agree well with the analytical results shown in Fig. 4. This implies that the stability of the orbit is controlled by Eq. (43).

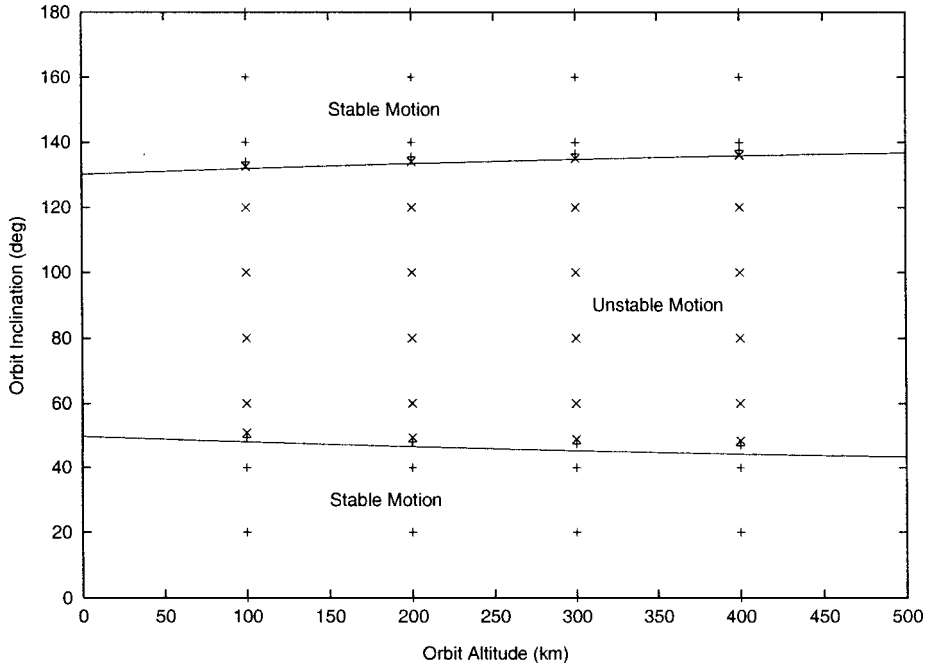

Fig. 4 Limiting inclination for stable orbital motion as a function of orbiter altitude; analytical results are represented by the solid line, for DPTRAJ results, the + indicates stable motion and the × indicates unstable (impacting) motion.

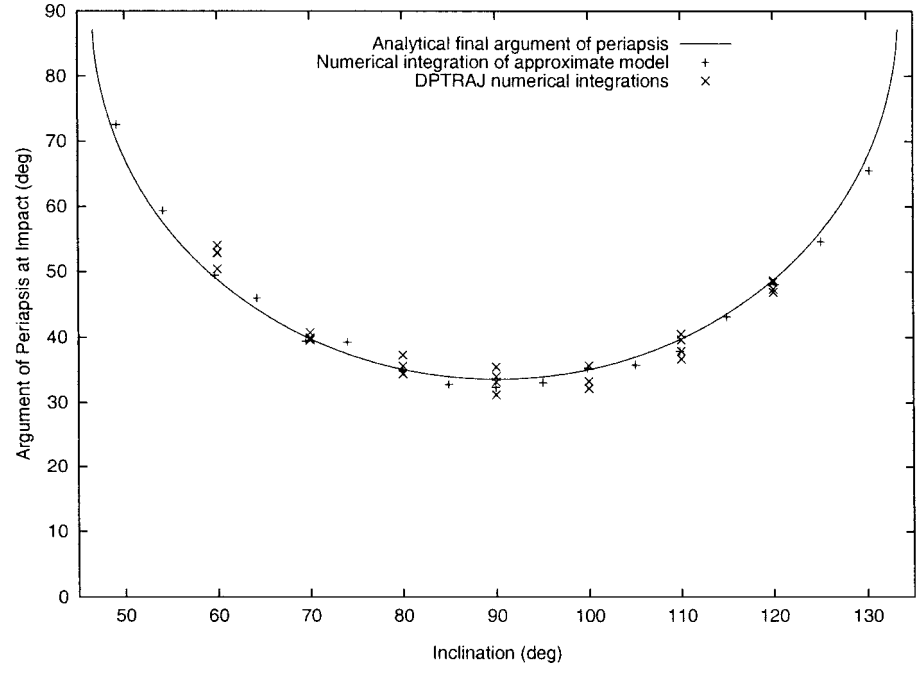

Fig. 5 Final value of argument of periapsis, comparison between analytical results, approximate model numerical results, and DPTRAJ results, computed with an initial altitude of 200 km and an initial eccentricity of 0.001; different DPTRAJ results correspond to runs made with varying initial conditions.

Final Value of Argument of Periapsis at Impact

To probe the accuracy to which the analytical theory correctly predicts the behavior of the argument of periapsis, we have performed a number of numerical integrations using the precision models contained in DPTRAJ and using the approximate, un-averaged model defined by Eq. (2), including the effect of the J_2 gravity term on the trajectory. In Fig. 5 we show the final argument of periapsis of the spacecraft at impact as a function of inclination (restricted to the range of unstable inclinations), comparing the numerical results with the analytical predictions. The DPTRAJ results were run over a number of different initial conditions, varying the initial longitude of the ascending node and argument of periapsis over their range of definition.

We note the very good agreement between the numerical solutions of the two models, indicating that our analysis has properly isolated the controlling force perturbations. Because the DPTRAJ runs also included the higher orders of the Europa gravity field, higher orders of the Jupiter gravity field, third-body perturbations from the other Galilean satellites, solar radiation pressure, and Europa atmospheric effects, it is interesting to note that the extremely simple force model used in our analysis properly captures the basic dynamics of this situation. Also, from this comparison, it is apparent that the averaging

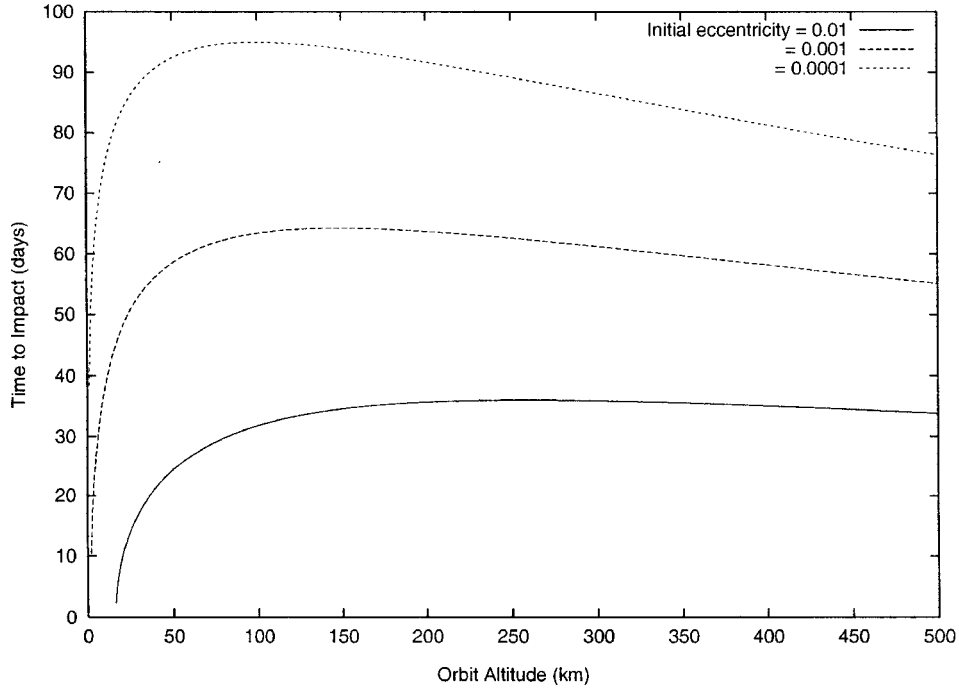

Fig. 6 Analytical results: variation of time to impact with initial altitude and initial eccentricity, computed for an inclination of 90 deg and an initial argument of periapsis of $\omega_0 = 0$; note that for a given combination, there is an altitude that maximizes the time to impact.

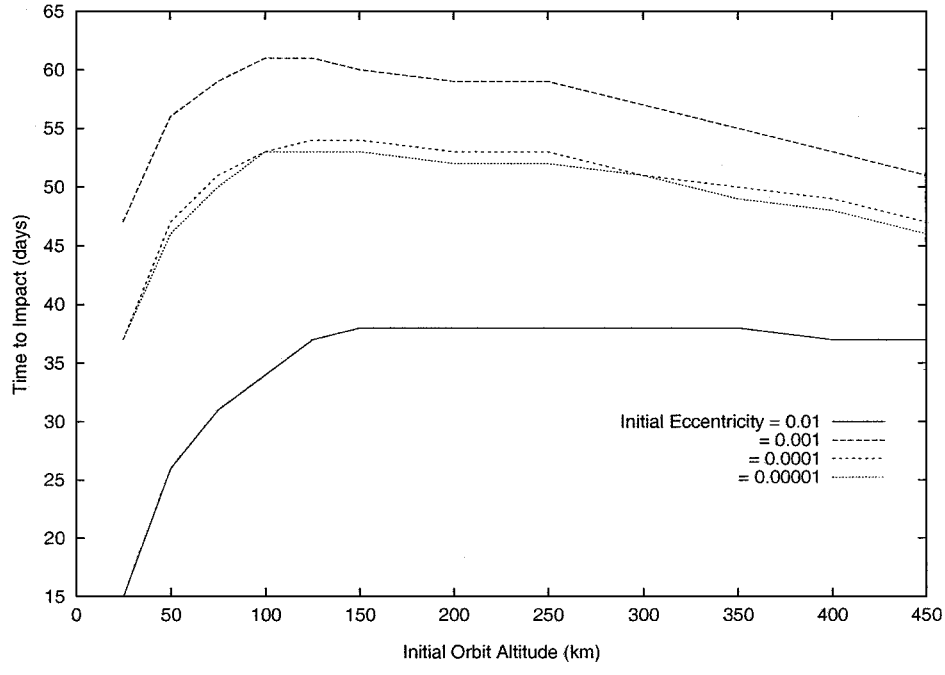

Fig. 7 DPTRAJ results: variation of time to impact with initial altitude and initial eccentricity, computed for an initial inclination of 90 deg and an initial argument of periapsis of 0 deg, saturation of the time to impact occurs for the smaller initial eccentricities due to the finite amplitude of oscillation of the eccentricity.

and small eccentricity assumptions made in the analysis are valid for the Europa orbiter because the analytical theory agrees well with the numerical results.

Time to Impact for an Unstable Orbit

The time to impact in Eq. (47) is a function of the initial orbit eccentricity, orbit altitude, orbit inclination, and argument of periapsis. To present these relations, we first fix the orbit inclination and argument of periapsis and allow the initial eccentricity and orbit altitude to vary (Figs. 6 and 7); then we fix the initial altitude and eccentricity and allow the initial inclination and argument of periapsis to vary (Figs. 8 and 9).

Figure 6 presents the time to impact as a function of initial eccentricity and altitude for the analytical results, contrasted with Fig. 7, which shows the time to impact for the DPTRAJ computations. In both cases, the initial inclination was 90 deg and the initial argument of periapsis was 0 deg. The basic shapes of the curves agree well between the two computations. The jump in impact time from the 0.01 case to the 0.001 case is a factor of approximately 1.6 for both cases. Also, the time to impact have maxima at the same approximate altitude for the cases of $e_0 = 0.01, 0.001$. In the DPTRAJ plot, the two cases where the initial eccentricity is close to zero are nearly identical. This is not surprising because the transient oscillations in eccentricity will dominate the averaged dynamics for

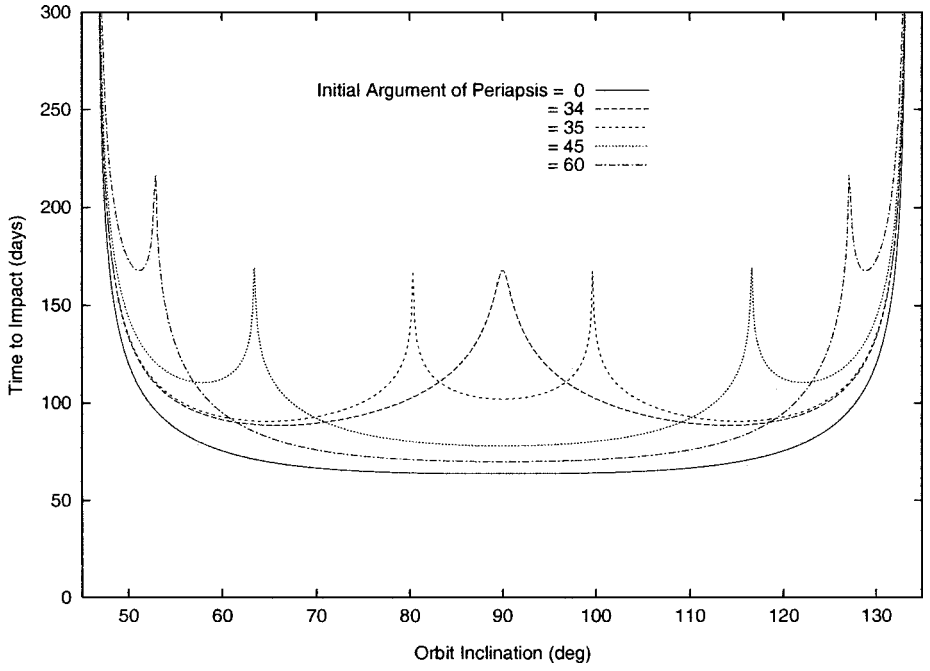

Fig. 8 Analytical results: variation of time to impact with initial inclination and argument of periapsis, computed assuming an initial altitude of 200 km and an initial eccentricity of 0.001; note that the time to impact ideally becomes infinite at the various peaks.

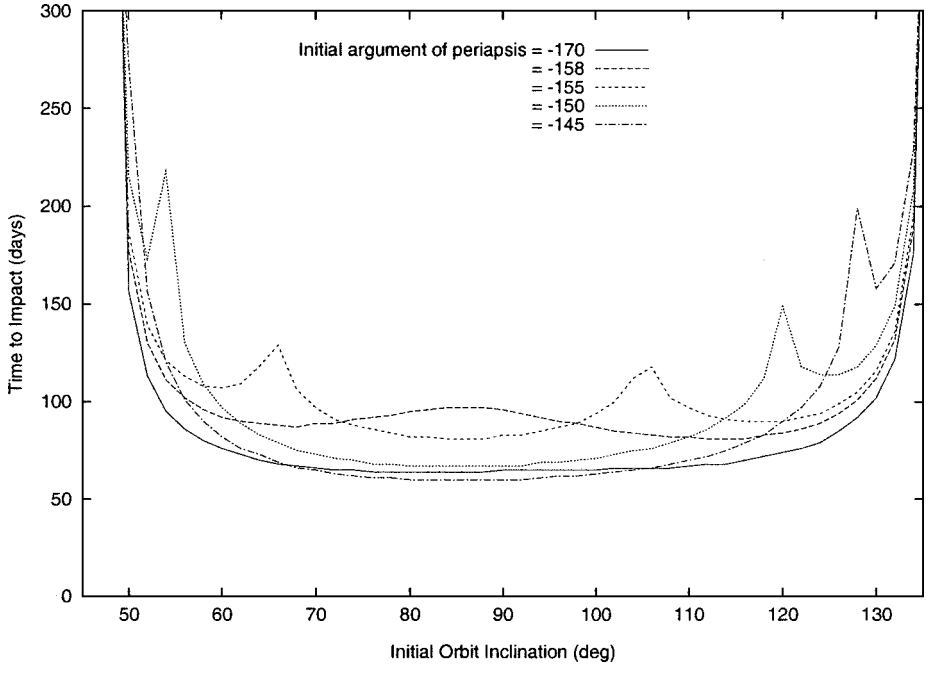

Fig. 9 DPTRAJ results: variation of time to impact with initial inclination and initial argument of periapsis, computed with an initial altitude of 200 km and an initial eccentricity of 0.001.

very small eccentricities. Analytic estimates show the amplitude of short-period eccentricity oscillations are on the order of 0.0001, which agrees with the implied numerical results from DPTRAJ in Fig. 7.

In Fig. 8, the time to impact is shown as a function of initial inclination and argument of periapsis, constrasted with Fig. 9, which shows the DPTRAJ-generated time to impact values. In Fig. 8 the time to impact peaks predicted earlier are clearly visible, corresponding to initial conditions along the stable manifold of the circular orbit-fixed point. Note that the structure of the plots in Figs. 8 and 9 agree well with each other, including the peaks in the time to impact for different combinations of inclination and argument of periapsis. However, the initial argument of periapsis values at which these peaks in time to impact occur are different between the two plots. The reason for the disagreement is that the time to impact, and, thus, the values of argument of periapsis at which the spikes occur, is dependent on the initial longitude of Jupiter about Europa. Additionally, the numerical solutions for the argument of periapsis usually have an initial period of circulation or libration before the angle becomes captured into the unstable manifold, which makes comparisons with initial averaged values difficult. For the DPTRAJ cases run here, the initial longitude of Jupiter is about 28° past the longitude of the ascending node of the spacecraft's orbit. Another set of DPTRAJ runs was performed with the initial longitude of Jupiter advanced by 90° (118° past the longitude of the ascending node of the spacecraft's orbit) and resulted in a different set of initial

argument of periapsis values at the time to impact spikes, although the overall qualitative shape of the plots were unchanged. The series of comparisons show that the analytical theory provides a correct qualitative description of the time to impact and, thus, can be used to direct investigations in how to maximize this time.

Extension to Other Planetary Satellite Orbiters

Given the simple form and the universality of the analytic results, it is fitting that they be applied to a larger range of solar system bodies. To perform these comparisons we took a published list of planetary satellites for which mass estimates exist[12] and computed all relevant constants for them.

The basic Hill assumptions only require a near-circular orbit for the planetary satellite and a relative mass ratio $(M_S/M_P)^{1/3} \ll 1$. These conditions are satisfied for almost all planetary satellites in the solar system, exceptions being Earth's moon and Pluto's moon, Charon, for which the mass ratios are not small. The averaging assumption made is that the ratio of the planetary satellite orbit mean motion over the spacecraft orbit mean motion is a small number, or $(N_S/n) \ll 1$. To enable comparison between different bodies we evaluate the spacecraft mean motion at the surface of the planetary satellite, designated as $n_S = \sqrt{(\mu_S/R_S^3)}$. This can be scaled to higher altitudes with the relation

$$n = n_S(1 + h/R_S)^{-\frac{3}{2}} \tag{54}$$

$$n \sim n_S(1 - 3h/2R_S) \tag{55}$$

The preceding conditions were computed for all planetary satellites of interest to check the applicability of the assumptions. Then, to compute a measure of the importance of this instability for near-polar orbits the characteristic exponent λ [Eq. (31)] of a polar orbit ($i = 90^\circ$) is computed for each body. For these computations, we assume $\epsilon = 0$ and $i = 90$ deg leading to $\alpha = -\frac{1}{5}$, which gives us a characteristic exponent of

$$\lambda = \left(3\sqrt{6}/4\right)(N_S/n_S)N_S \tag{56}$$

$$\lambda \sim 1.837(N_S/n_S)N_S \tag{57}$$

Thus, whenever the condition $(N_S/n_S) \ll 1$ holds, the condition $\lambda/N_S \ll 1$ should also hold. This assumption was explicitly made when the second averaging was performed for elimination of the longitude of the ascending node. Of specific interest is the characteristic time of the eccentricity instability, $\tau = 1/\lambda$. In general, the eccentricity will increase by an order of magnitude after $e \sim 2.718$ characteristic times. From these relations, we see that the characteristic time of the instability is a function only of the planet's mass, the satellite's orbit radius, and the ratio of the satellite's mass with the planet's mass and the ratio of the satellite's physical radius with the satellite's orbit radius. If we express the characteristic time in terms of satellite orbital revolutions about the planet, then we find

$$\frac{\tau}{(2\pi/N_S)} = \left(2/3\pi\sqrt{6}\right)(n_S/N_S) \tag{58}$$

and the characteristic time measured in satellite orbit periods is only a function of the ratio of mass parameters and the ratio of the satellite's physical radius with its orbital radius.

Table 1 presents the results of these computations for orbiters about all of the solar system bodies of interest. For each planet with satellites, we list the moons, the mass ratios $(M_S/M_P)^{1/3}$, the averaging conditions (N_S/n_S), the orbit period of the moons $(2\pi/N_S)$, and the characteristic times of the instability at the surface of the planetary satellite (τ_S). We assume that for the theory to be properly applicable requires $(M_S/M_P)^{1/3} < 0.1$ and $(N_S/n_S) < 0.1$, which means that ignored terms in the force function are of the order of 0.01 and that the periods of the orbiter and the satellite are at least an order of magnitude apart. When these conditions are violated, the modeling assumptions will begin to break down, and coupling between the time variations can begin to become important. We include, for completeness, some planetary satellites of interest that do not satisfy these conditions. We do not include any planetary satellites with characteristic instability times greater than a few years (other than the Earth's moon). From Table 1, we see that this instability can be a signifcant concern for most planetary satellite orbiters. Of interest, however, is that the instability for a Titan orbiter is relatively mild, on the order of 220 days, which means that it may only become significant over longer periods of time and that it may be easily controlled by occasional maneuvers.

Table 1 Summary of approximation conditions and validity, planetary satellite orbit period, and orbiter characteristic instability time for solar system planetary satellites

Satellite	Mass ratio $(M_S/M_P)^{1/3}$	Mean motion ratio N_S/n_s	Satellite orbit period $2\pi/N_S$, day	Characteristic instability time τ_S, day
		Earth		
Moon	0.231[a]	0.00274	27.45	880.19
		Mars		
Deimos	0.0014	0.0806	1.26	1.35
Phobos	0.0025	0.3328[b]	0.32	0.08
		Jupiter		
Io	0.036	0.04123	1.77	3.72
Europa	0.0293	0.0225	3.55	13.66
Ganymede	0.0427	0.0138	7.15	44.87
Callisto	0.0384	0.00604	16.69	239.11
Amalthea	0.0015	0.1931[b]	0.497	0.22
Thebe	0.00073	0.1763[b]	0.676	0.33
Adrastea	0.00021	0.2089[b]	0.299	0.12
Metis	0.00037	0.2762[b]	0.296	0.09
		Saturn		
Mimas	0.0043	0.1214[b]	0.943	0.67
Enceladus	0.0051	0.0944	1.371	1.26
Tethys	0.0109	0.0669	1.888	2.44
Dione	0.0123	0.042	2.737	5.64
Rhea	0.0164	0.0263	4.518	14.85
Titan	0.0619	0.00627	15.946	220.28
Hyperion	0.0031	0.00548	21.28	336.19
		Neptune		
Triton	0.0593	0.0163	5.867	31.20
		Uranus		
Ariel	0.0249	0.04225	2.525	5.18
Umbriel	0.0238	0.0281	4.157	12.82
Titania	0.0343	0.0121	8.705	62.28
Oberon	0.0326	0.008	13.48	145.81
Miranda	0.0092	0.0893	1.408	1.36
		Pluto		
Charon	0.603[a]	0.0112	6.307	48.70

[a]Formally violates mass restriction for the application of Hill's approximation.
[b]Formally violates our frequency condition for application of the second averaging assumption.

Conclusions

We have developed an analytic theory that predicts and parameterizes the instability of low-altitude orbiters about planetary satellites. Our model is based on a secular theory of motion in the Hill equations of motion with the secular effect of the satellite oblateness added in. The theory predicts that low-altitude, nearly circular orbits will suffer an exponential growth in their eccentricities for a range of inclinations centered about 90 deg, precise values depending on the model parameter values. If the satellite is modeled as a point mass, the unstable inclinations range from 39.23 to 140.77 deg. If the satellite has a strong oblateness contribution and moves in a relatively slow orbit about the primary, the unstable inclinations are limited to an interval centered on the critical inclinations for the oblate satellite case, which are at 63.43 and 116.56 deg. For the case of unstable motion, the theory provides predictions of time to impact as a function of the initial orbit conditions. From this analysis, special initial conditions are found that can prolong the time to impact significantly and that suggest some simple orbit control techniques which can prolong the life of an unstable orbiter indefinitely. Application of the results are made to all planetary satellites of potential interest in the solar system. From these comparisons, we find that this orbital instability is present in all of the major

planetary satellites of interest. The theory is compared with precision numerical integrations for the case of the Europa orbiter and is able to predict stability regions and variation of time to impact as a function of initial conditions.

Appendix: Computational Models

The numerical values of constants used in the analysis of the Europa orbiter spacecraft are given. Additionally, an explicit description of the precision numerical integrations performed by DPTRAJ are given.

Europa Models and Parameters used in the Analysis

For the mathematical analysis of this problem, only the force models and parameters that provide a major perturbation are used. These include the tidal effect of Jupiter on a Europa orbiter and the effect of the Europa oblateness on the low-altitude orbiter. Because Europa is in a tidally locked rotation state with its parent body, Jupiter, we assume that its rotation period and orbit period are equal for the simplified model. We show that this simple set of force models is able to capture the observed instabilities in the orbiter. Table A1 provides a list of the values used in the analysis.

DPTRAJ Models and Parameters

The orbit dynamics of the spacecraft are also modeled using the DPTRAJ program. DPTRAJ is a high-accuracy trajectory computation program used in the navigation and design of space missions.[13] It is an accurate and general trajectory program for spacecraft due to its ability to model all relevant force perturbations found in the solar system to high levels of precision. To simulate the real orbit dynamics of the Europa orbiter, we use this program with a complete suite of force models. In the runs made for this analysis, these force models included gravitational perturbations from the sun and planets, the Galilean satellites (Io, Ganymede, Callisto, and Europa, of course), J_2 and J_4 for Jupiter, and the Europa gravity field up to second degree and order. Also incorporated are the nongravitational perturbations of the Europa atmosphere and solar radiation pressure.

Table A1 Europa orbit stability study model assumptions

Parameter	Symbol	Value	Units
Europa gravitational parameter	μ_E	3.201×10^3	km^3/s^2
Jupiter gravitational parameter	μ_J	1.267×10^8	km^3/s^2
Mass ratio	$(\mu_E/\mu_J)^{1/3}$	0.029	——
Europa radius	R_E	1565	km
Europa oblateness	J_2	1051.315	km^2
Europa orbit period	T_E	3.552	days
Europa orbit rate	N_E	2.05×10^{-5}	rad/s
Orbiter nominal altitude	h	200	km
Orbiter nominal period	T	2.28	h
Orbiter nominal orbit rate	n	7.66×10^{-4}	rad/s

Acknowledgments

D. J. Scheeres thanks L. A. D'Amario of the Jet Propulsion Laboratory, California Institute of Technology for initially bringing the instability of the Europa orbiter near-polar orbits to our attention. The work described was funded by the Telecommunications and Mission Operations Directorate Technology Program and Outer Planets/Solar Probe Project by grants from the Jet Propulsion Laboratory, California Institute of Technology, which is under contract with NASA.

References

[1]Marchal, C., *The Three-Body Problem*, Elsevier, New York, 1990, p. 63.

[2]Wintner, A., *The Analytical Foundations of Celestial Mechanics*, Princeton Univ. Press, Princeton, NJ, 1947, pp. 379–384.

[3]Scheeres, D. J., "The Restricted Hill Four-Body Problem with Applications to the Earth–Moon–Sun System," *Celestial Mechanics*, Vol. 70, No. 2, 1998, pp. 75–98.

[4]Hénon, M., "Numerical Exploration of the Restricted Problem. V.," *Astronomy and Astrophysics*, Vol. 1, No. 1, 1969, pp. 223–238.

[5]Chauvineau, B., and Mignard, F., "Dynamics of Binary Asteroids. I.," *Icarus*, Vol. 83, No. 2, 1990, pp. 360–381.

[6]Hamilton, D. P., and Krivov, A. V., "Dynamics of Distant Moons of Asteroids," *Icarus*, Vol. 128, No. 1, 1997, pp. 241–249.

[7]Johannesen, J. R., and D'Amario, L. A., "Europa Orbiter Mission Trajectory Design," American Astronautical Society Paper 99-360, 1999.

[8]Brouwer, D., and Clemence, G. M., *Methods of Celestial Mechanics*, Academic, New York, 1961, pp. 289, 337.

[9]Scheeres, D. J., "On Symmetric Central Configurations with Application to Satellite Motion About Rings," Ph.D. Thesis, Dept. of Aerospace Engineering, Univ. of Michigan, Ann Arbor, MI, 1992, Appendix E.

[10]Moulton, F. R., *An Introduction to Celestial Mechanics*, Macmillan, New York, 1935, p. 360.

[11]Danby, J. M. A., *Fundamentals of Celestial Mechanics, 2nd Ed.*, Willmann–Bell, Richmond, VA, 1992, pp. 343–346.

[12]Seidelmann, P. K. (ed.), *Explanatory Supplement to the Astronomical Almanac*, University Science Books, Mill Valley, CA, 1992, pp. 706–711.

[13]Ekelund, J. E., "DPTRAJ-ODP User's Reference Manual, Volume 1," Jet Propulsion Lab., California Inst. of Technology Internal Memo, JPL 642-3405-DPTRAJ-ODP, Pasadena, CA, 1996.